FINAL TECHNICAL REPORT

USGS AWARD G19AP00059

Earthquake rupture propagation into creeping areas of the San Andreas Fault

Principal Investigator: Nadia Lapusta, California Institute of Technology
1200 E. California Blvd., Pasadena, CA 91125
(626) 395-2277, Fax: (626) 568-2719, lapusta@caltech.edu

Term covered by the award: 5/15/19 to 5/14/20

Acknowledgement of Support and Disclaimer

This material is based upon work supported by the U.S. Geological Survey under Grant No. G19AP00059. The views and conclusions contained in this document are those of the authors and should not be interpreted as representing the opinions or policies of the U.S. Geological Survey. Mention of trade names or commercial products does not constitute their endorsement by the U.S. Geological Survey.

Abstract

The Parkfield section of the San Andreas fault is a well-instrumented natural laboratory that displays the full range of slip behaviors: relatively large, quasi-periodic Mw 6 events, small repeating earthquakes, seismic tremors, and creeping regions. The uniqueness of this area has been exploited in a number of studies, including the San Andreas Fault Observatory at Depth (SAFOD) drilling project. Small repeating earthquakes are used to address an increasingly richer array of problems, from fault creeping velocities and postseismic slip to earthquake interaction and stress drops.

Our previous studies supported by USGS have resulted in fault models capable of reproducing a number of observations at Parkfield, such as scaling of small repeating earthquakes, their response to postseismic slip, and quasi-periodic recurrence of Mw 6 events and the associated post- and interseismic slip. Our models resulted in estimates of fault zone properties consistent with the observed behaviors. We have also explained the difference in the microseismicity patterns on the Parkfield segment and nearby segments by the deeper propagation of large earthquakes in the latter case due to enhanced dynamic weakening. Our studies show that the crucial aspect in these phenomena is the interaction of seismic and aseismic slip. To model such interaction while producing realistic behavior that can be compared to observations, one needs to use the modeling approach that fully reproduces the inertial, stress-concentrating effects during seismic events, while seamlessly resolving the transition between seismic and aseismic slip, as our modeling methodology is capable of doing.

With this award, we continued to use our models together with Parkfield observations to further constrain fault properties and earthquake physics by investigating the following two topics: (1) Fault properties in the creeping segment needed to match the irregularity of repeating earthquake sequences and (2) the possibility of dynamic rupture propagating through the creeping segment, due to enhanced dynamic weakening in the form of shear-heating-induced thermal pressurization of pore fluids.

Observations indicate that the seismic moment, recurrence times, and interaction of repeating sequences is Parkfield are irregular. We have focused our research on the reproducing the variability of the well-studied LA and SF repeaters. We find that models with fractal shapes of VW patches produce repeating sequences with more variability than the often-used models with circular patches, resulting in variability comparable to that of the SF-LA sequences. We also find that the variability in models with

simple, circular patches depends on the properties of the surrounding VS region, with smaller values of velocity-strengthening leading to more variable behavior that is also comparable to that of the SF-LA sequences. The two findings combined suggest that there could be many model setups that reproduce the observed variability. Note that other properties are likely to be heterogeneous as well. One potential way forward is to develop a suite of models with different types of heterogeneity that can reproduce the available observations and then study whether there are other observables that would be able to distinguish between the possible models. We used the developed heterogeneous models with the fractal shapes of the VW regions to study the effect of small-scale heterogeneity and find that only heterogeneity smaller than the governing length scale, which is the nucleation size in our models, does not affect the key features of the response, such as variability or range of triggering times. We plan to investigate this conclusion through further modeling.

Our modeling also focused on identifying the range of physical properties of the creeping segment for which large enough dynamic rupture approaching from the Carrizo segment would penetrate into or even propagate through the creeping segment. Using a simplified 2D model, we find that there is a range of dynamic weakening parameters for which Mw 6 events arrest in the creeping section, but larger, Mw 7.2 style events are able to propagate partially or completely through. Such ruptures would allow for the linking of the northern and southern parts of the San Andreas, allowing for much larger earthquakes. The identified sets of properties will serve as starting points for more sophisticated future studies in 3D models.

Our studies have advanced our understanding of fault slip, earthquake nucleation, and triggering and of the relevant properties of parts of the SAF. They will eventually contribute to the evaluation of seismic hazard in California. The research is well aligned with the USGS Priority Topics in Research on Earthquake Physics.

1. Models of fault slip with rate-and-state friction and dynamic weakening

Our previous studies supported by USGS have resulted in fault models capable of reproducing a number of observations at and around Parkfield, such as scaling of small repeating earthquakes, their response to postseismic slip, relatively large stress drops and interaction of the LA and SF repeaters, quasi-periodic recurrence of the Mw 6 events and the associated post- and interseismic slip (Chen and Lapusta, 2009; Chen et al., 2010; Barbot et al., 2012; Lui and Lapusta, 2016, 2018). The models and their extensions have been used to explore the potential for and consequences of deeper penetration of earthquake rupture into creeping fault extensions and the potential for dynamic rupture to propagate through creeping segments (Noda and Lapusta, 2013; Jiang and Lapusta, 2016, 2017).

Our models include two aspects of earthquake source physics that have been gaining acceptance and validation through laboratory experiments and comparison of earthquake models with observations.

The first one is the rate-and-state nature of fault friction at low, aseismic slip rates, conclusively documented in laboratory experiments and used to reproduce, both qualitatively and quantitatively, a number of earthquake-source observations (Dieterich, 2007; Scholz, 1998). Our previous studies supported by USGS have shown that the standard logarithmic rate and state formulations (Dieterich, 1979, 1981; Ruina, 1983; Blanpied et al., 1991, 1995; Beeler et al., 1994; Marone, 1998) allow us to match a number of basic observations regarding repeating earthquakes in the creeping section and quasi-periodic Mw 6 events (Chen and Lapusta, 2009; Chen et al., 2010; Barbot et al., 2012). Such laws express the dependence of frictional shear strength τ_f on the effective normal stress $\bar{\sigma}$, slip rate V (which we also call slip velocity), and evolving properties (state) of the contact population represented by the state variable θ, through:

$$\tau_f = \bar{\sigma} f = (\sigma - p)[f_o + a\ln(V/V_o) + b\ln(V_o\theta/L)],$$
$$\frac{\partial\theta}{\partial t} = 1 - \frac{V\theta}{L} \text{ or } \frac{\partial\theta}{\partial t} = -\frac{V\theta}{L}\ln\frac{V\theta}{L} \text{ or } \frac{\partial\theta}{\partial t} = \exp\left(-\frac{V}{V_c}\right) - \frac{V\theta}{L}\ln\frac{V\theta}{L}, \quad (1)$$

where σ is the normal traction, p is the pore pressure, f_o, V_o, a, b, and L are rate and state parameters, with L being the characteristic slip for state variable evolution, and V_c is the cut-off velocity of the order of 10^{-8} m/s. In these laws, the rate and state features result in small variations (of the order of 1-10%) from the baseline frictional strength given by $\bar{\sigma} f_o$. Despite being small, these variations are fundamentally important for physically and mathematically meaningful stability properties of frictional sliding (e.g., Rice, Lapusta, and Ranjith, 2001). In the steady state, $(a - b)$ is the rate-and-state parameter that can be used to model both stable, velocity-strengthening (VS) fault segments ($a - b > 0$) and potentially seismic, velocity-weakening (VW) fault segments ($a - b < 0$). Equations (1) give several proposed forms for the state variable evolution; which of these laws does a better job of representing the range of available experimental results and serves as the best simplified representation of the state variable evolution for simulations of long-term slip is an active area of research (Kato and Tullis, 2001; Hori et al., 2004; Rubin and Ampuero, 2005; Bayart et al., 2006; Ampuero and Rubin, 2008; Bhattacharya et al., 2015). We have used all of these forms in our modeling, and the obtained results are qualitatively, and often quantitatively, similar. We will mostly use the aging form, since it incorporates the physically sound notion of friction increase in stationary contact, a feature required for the production of slip pulses (Perrin et al., 1995), and it is the easiest to properly resolve numerically. However, we will verify the robustness of the important results by using the other two forms of the state variable evolution.

The second emerging property of the earthquake source is additional substantial fault weakening at seismic slip rates. While theories of such dynamic weakening have a long history (Sibson, 1973), relatively recent laboratory confirmations of this phenomenon (Tsutsumi and Shimamoto, 1997; Tullis, 2007 and references therein) have put this notion on the earthquake science map. We have incorporated shear heating dynamic weakening mechanisms, such as flash heating and thermal pressurization, into our simulations, including those of repeating earthquakes (Lui and Lapusta, 2017). Dynamic weakening of creeping regions allows them to sustain seismic slip (Noda and Lapusta, 2010, 2013; Jiang and Lapusta, 2016, 2017). One shear-heating weakening mechanism with laboratory support is flash heating (e.g., Goldsby and Tullis, 2003, Beeler and Tullis, 2003, Rice, 2006, Beeler et al. 2008, Goldsby and Tullis, 2011), in which tips of contacting fault gouge grains heat up and weaken. Such weakening can be activated even for very small slips of the order of 10-100 microns if the shear strain rate is high enough. Another relevant mechanism is pore fluid pressurization (e.g., Sibson, 1973; Andrews, 2002; Bizzarri and Cocco, 2006a,b; Rice, 2006; Noda et al., 2009), in which rapid shearing raises the temperature and hence pore fluid pressure, lowering the effective normal stress and hence frictional resistance. To include flash heating and/or pore pressurization into our models, we modify the rate and state formulation (1) to

$$\tau_f = \bar{\sigma} f = (\sigma - p)\left[\frac{f_o - f_w + a\ln(V/V_o) + b\ln(V_o\theta/L)}{1 + L/\theta V_w} + f_w\right], \tag{2}$$

where V_w is the characteristic slip velocity at which flash heating starts to operate, f_w is the residual friction coefficient, and pore pressure p could be evolving due to shear heating as discussed below. Based on laboratory experiments and flash heating theories, V_w is of the order of 0.1 m/s. Selecting much larger values of V_w than the seismic slip rates of the order of 1-10 m/s would effectively disable the additional weakening due to flash heating. The coupled temperature and pore pressure evolution is calculated by (Rice, 2006 and references therein, Noda et al., 2009, Noda and Lapusta, 2010):

$$\frac{\partial T}{\partial t} = \alpha_{th}\frac{\partial^2 T}{\partial y^2} + \frac{\omega(y)}{\rho c}, \quad \frac{\partial p}{\partial t} = \alpha_{hy}\frac{\partial^2 p}{\partial y^2} + \Lambda\frac{\partial T}{\partial t}, \quad \omega = \tau V\frac{\exp(-y^2/2w^2)}{\sqrt{2\pi}w} \tag{3}$$

where y is the space coordinate normal to the fault, T is the temperature, α_{th} and α_{hy} are the thermal and hydraulic diffusivities, $\omega(y)$ is the heat generation rate the integral of which over the width w of the shearing layer equals to $\tau_f V = \tau V$, ρc is the specific heat, Λ is pore pressure change per unit temperature change under undrained condition. (Note that this formulation can also include inelastic dilatancy, as an

additional term in the equation for the pore pressure evolution.) The heat source, $\omega(y)$, is distributed in a narrow shear zone around the fault. The standard assumption is to take this term to represent the effect of uniform sliding in the fault zone of thickness w.

In our simulations, spontaneous long-term slip history of a fault governed by constitutive relations (1-3) and embedded into an elastic half-space is determined using the 3D simulation methodology of Lapusta and Liu (2009) and Noda and Lapusta (2010) developed with prior NSF and USGS support. The methodology incorporates slow tectonic-type loading and all dynamic effects of self-driven dynamic rupture. The algorithm allows us to treat accurately long deformation histories and to calculate, for each earthquake episode, initially quasi-static accelerating slip (nucleation process), the following dynamic rupture break-out and propagation, postseismic response, and ongoing slippage throughout the loading period in creeping fault region.

2. Modeling the variability of repeating earthquake sequences on rate-and-state interfaces: realistic shapes of source patches vs. properties of the creeping region

The creeping section next to Parkfield contains a number of repeating earthquakes sequences, which are events with highly correlated seismograms that translate into similar moment magnitudes and nearly identical locations. Small repeating earthquakes occur on a number of other faults and their observations have been used to study various aspects of earthquake physics and mechanics (e.g., Ellsworth and Dietz, 1990; Vidale et al., 1994; Marone et al., 1995; Nadeau and Johnson, 1998; Schaff et al., 1998; Nadeau and McEvilly, 1999, 2004; Bürgmann et al., 2000; Beeler et al., 2001; Sammis and Rice, 2001; Igarashi et al., 2003; Imanishi et al., 2004; Nadeau et al., 2004; Schaff and Beroza, 2004; Matsubara et al., 2005; Allmann and Shearer, 2007; Chen et al., 2007; Rubinstein et al., 2012).

Many properties of these sequences have been successfully modeled as repeating ruptures of circular VW patches embedded into a VS region (e.g., Chen and Lapusta, 2009; Lui and Lapusta, 2018). One of the most interesting observations about the repeaters is their scaling $T \sim M_0^{0.17}$ (Nadeau and Johnson, 1998) between the recurrence time T and seismic moment M_0, which is significantly different from $T \sim M_0^{1/3}$, the scaling that results in a simple conceptual model in which seismic events release all accumulated slip deficit $V_L T$ (where V_L is the long-term creeping velocity of the segment) and have stress drop independent of the seismic moment. Moreover, the recurrence time for the smallest repeaters is significantly longer than expected for moderate stress drops of 10 MPa, translating into stress drops of 3-4 GPa (3000-4000 MPa) for the simple model mentioned above (Nadeau and Johnson, 1998). Our models reproduce the observed scaling due to significant aseismic slip at the location of seismic events, with the fraction of aseismic slip being larger for smaller events. This makes sense based on stability studies of VW faults (Rice and Ruina, 1983; Rice et al., 2001; Rubin and Ampuero, 2005), since small enough VW patches would be below the nucleation size and hence completely aseismic. Our models confirm the idea of Beeler et al. (2001) that the observed scaling may be due to the presence of aseismic slip.

Our detailed modeling has been focused on the LA and SF repeaters, the main targets of the SAFOD experiment (Figure 1; Lui and Lapusta, 2016, 2018; Sudhir and Lapusta, 2020). These repeaters are characterized by two more interesting observations. The first one is their interaction before 2004 Parkfield event, with the LA events occurring within 24 hours of the SF events. The second is their relatively large stress drops, of 25-60 MPa on average, with local stress changes potentially as large as 90 MPa (Abercrombie, 1995, 2014; Nadeau and Johnson, 1998; Sammis et al., 1999; Dreger et al., 2007). We have shown that two types of models reproduce the observations of relatively large stress drops. In one type of models, the large stress drops are achieved by enhanced dynamic weakening due to thermal pressurization of pore fluids; with the narrowest shear zones and smallest hydraulic diffusivities cited in Rice (2006), the thermal pressurization is significant even for the Mw 2 events considered here. In the other model, a much elevated value of normal stress is assumed at the location of the repeaters (e.g., due to a flattened "bump" on the slipping surface). Both models can approximately reproduce relatively large average stress drops of ~30 MPa with local changes up to 80 MPa, along with the average moment and

recurrence time, as well as the qualitative aspects of interaction between two sequences, with LA events occurring tens of seconds to hours after the SF ones. The interaction occurs mainly due to the effect of postseismic slip between the two patches (Lui and Lapusta, 2016, 2018). In our work under this project, we used the second type of models to represent the repeaters.

Observations show that even these repeating events are not identical, with significant differences in seismic moment and recurrence time; furthermore, the repeating events are neither time-predictable nor slip-predictable (Rubinstein et al, 2012; Figure 1), which basically means, counter intuitively, that smaller recurrence intervals often follow larger events and that smaller events often follow large recurrence intervals. The time progression of moment magnitudes of the LA-SF repeater sequence indicates significant variability within the sequences (Figure 1a). The LA events occurred shortly after the SF events, pointing to strong interaction between the two sequences, with inter-event times spanning from few seconds to months. It would be important to understand how much this interaction between the two repeater sources affects their variability of occurrence. The triggering times of the LA events by the SF events (Figure 1b) span a wide range, from a significant (0.25) to a tiny (10^{-6}) fraction of the recurrence interval. The time- and slip-predictability plots for the LA-SF repeating sequences (Figure 1c) further visualize their variability. Some of this variability can be explained by complex slip dynamics in our models (Lui and Lapusta, 2018) even for relatively simple distributions of friction properties, such as circular VW areas. In part, aseismic slip that occurs between seismic events can release different amounts of fault stress, complicating the repeating sequence.

Here, we focus on reproducing the observed level of variability and how fault heterogeneity is reflected in the variability (Sudhir and Lapusta, manuscript in preparation). The presence of many repeating sequences in the creeping segment suggests that the friction properties in the area may be heterogeneous in general. As a first step, we consider the effect of the source patch shape, moving from the circular shape to realistic, fractal-based shapes. We consider property distributions motivated by truncated fractal distributions used to characterize the spatial complexity of inferred earthquake slip and fault nonplanarity (e.g., Mai and Beroza, 2002, Brodsky et al., 2011). Such two-dimensional distributions can be characterized by their power spectral density, $P(k) \propto 1/k^{2(1+H)}$, where k is a dimensionless wave number and H is the Hurst exponent. H controls the decay of the PSD at high frequencies, and it is taken to be unity (self-similar distribution) in this study. The PSD decays with a power law beyond a corner wave number, k_c , which is related to the characteristic source dimension (Figure 2). k_c and H are the two parameters that characterize the field. For a given set of parameters, we can generate infinitely many realizations of the random distributions, by convolving with differently seeded random matrices. Amongst these, we choose the realization shown in Figure 2b as a starting point, due to the serendipitous existence of two dominant high-intensity patches, which could translate into the two repeater sources, when converted into frictional property distributions. We translate the random field values into a pattern of VW and VS friction properties (Figure 2a). The slip velocity snapshots from the representative model (Figure 2a) show a typical triggering sequence between the two repeaters (Figure 3). In part, the scaling behavior of the repeater sequences observed at Parkfield is reproduced (Figure 4). The double-patch models used to study the effect of patch shape and perturbing patches and the naming convention they follow are shown in Figure 5.

We find that models with fractal shapes of VW patches produce repeating sequences with more variability than the models with circular patches (Figure 6-7), resulting in variability of triggering times comparable to that of the SF-LA sequences. We can further increase the variability of the slip patterns by adding perturbing sub-critical patches which arise naturally from the underlying fractal distribution (F1p-D; Figure 5).

We also find that the variability in models with simple, circular patches depends on the properties of the surrounding VS region, with smaller values of velocity-strengthening leading to more variable behavior that is also comparable to that of the SF-LA sequences (Figure 8).

The two findings combined suggest that there could be many model setups that reproduce the observed variability in moments, recurrence times, and triggering times, as one combines the complexity of the shape of the patches and the value of the VS of the surrounding medium. Hence the variability and

the range of triggering times cannot be used to individually constrain the VS properties or the shape of the VW patches, as we hoped. Note that other fault properties could be heterogeneous as well, such as the normal stress, the values of VW within the VW region etc. One potential way forward is to develop a suite of models with different types of heterogeneity that can all reproduce the available observations and then study whether there are other observables that would be different between the possible models.

We have used the developed heterogeneous models with the fractal shapes of the VW regions to study the effect of small-scale heterogeneity. To create models smoother at smaller scales, we cut the power spectral density of the underlying fractal distribution above a wavenumber threshold, $\mathrm{k_{cut-off}}$, resulting in the removal of frequencies higher than that threshold and the distribution being smoother at smaller scales (Figure 9). The resulting slip behavior is different for all models (Figure 10), but it starts to be qualitatively different, for example in terms of the resulting range of the triggering times, only for sufficiently smooth models. The triggering times for $\log_{10}\mathrm{k_{cut-off}} = 0.95$ to $\log_{10}\mathrm{k_{cut-off}} = -0.56$ show realistic triggering time ranges. For $\log_{10}\mathrm{k_{cut-off}} = -0.73$ and lower wavenumber thresholds, however, with most of the fractal features smoothed on scales comparable to h^*, the short triggering times (1-100 s) vanish, diverging from observations. Our hypothesis is that heterogeneity on the scales small compared to the governing length scales, which is the nucleation size h^* for this specific problem, are not be important for the qualitative features of the response, something that we plan to investigate further.

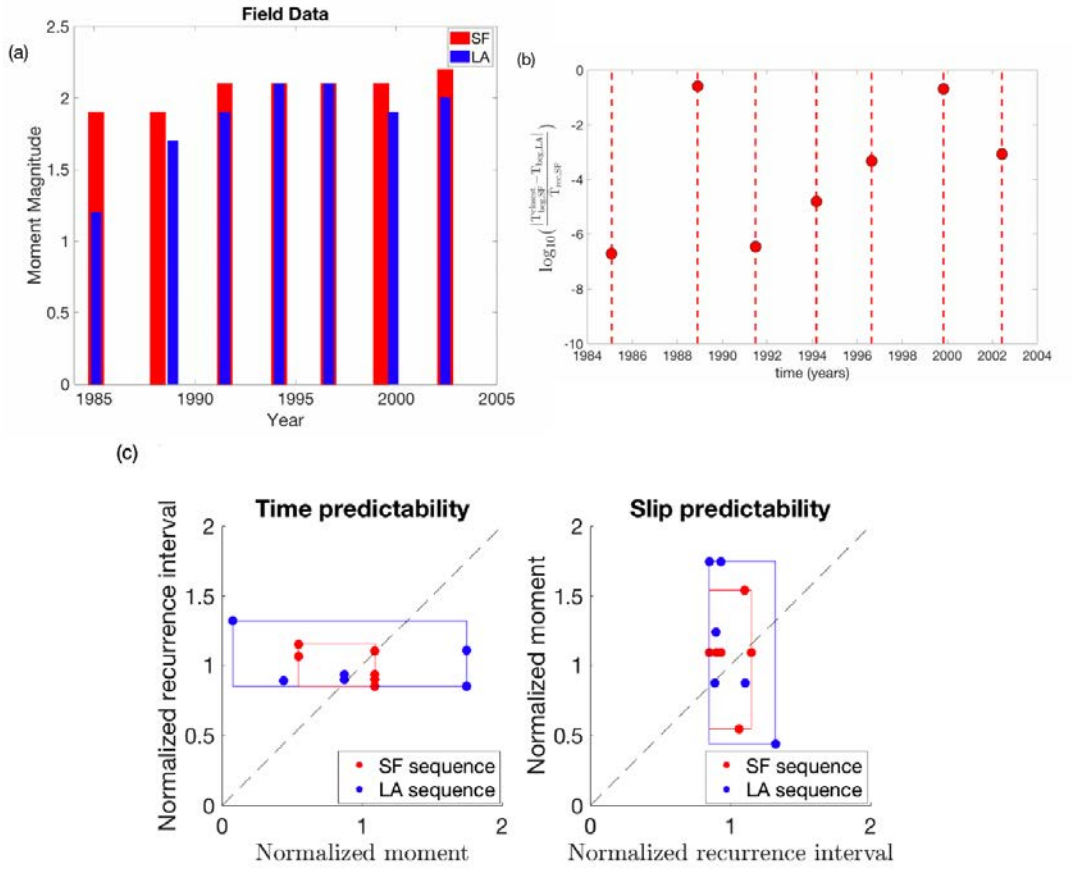

Figure 1: Variability of the SF and LA repeating sequences. (a) Time progression of moment magnitudes before the 2004 M6 Parkfield earthquake. The LA events (blue bars) consistently happen soon after the SF events (red bars), indicating a strong interaction between the two sequences, with inter-event times spanning from seconds to months. (From updated catalog, Waldhauser, 2008.) (b) Triggering times for the 7 SF-LA event pairs before 2004, plotted on a log-scale normalized with respect to the mean recurrence time of SF sequence. (c) Seismic moment vs. the following recurrence time interval (left) and recurrence time interval vs. the seismic moment of the following event (right), which test time predictability and slip predictability, respectively, for the 6 recurrence periods of SF and LA sequences. The axes are normalized with respect to the mean quantities. The red and blue rectangles illustrate the variability of SF and LA events, respectively.

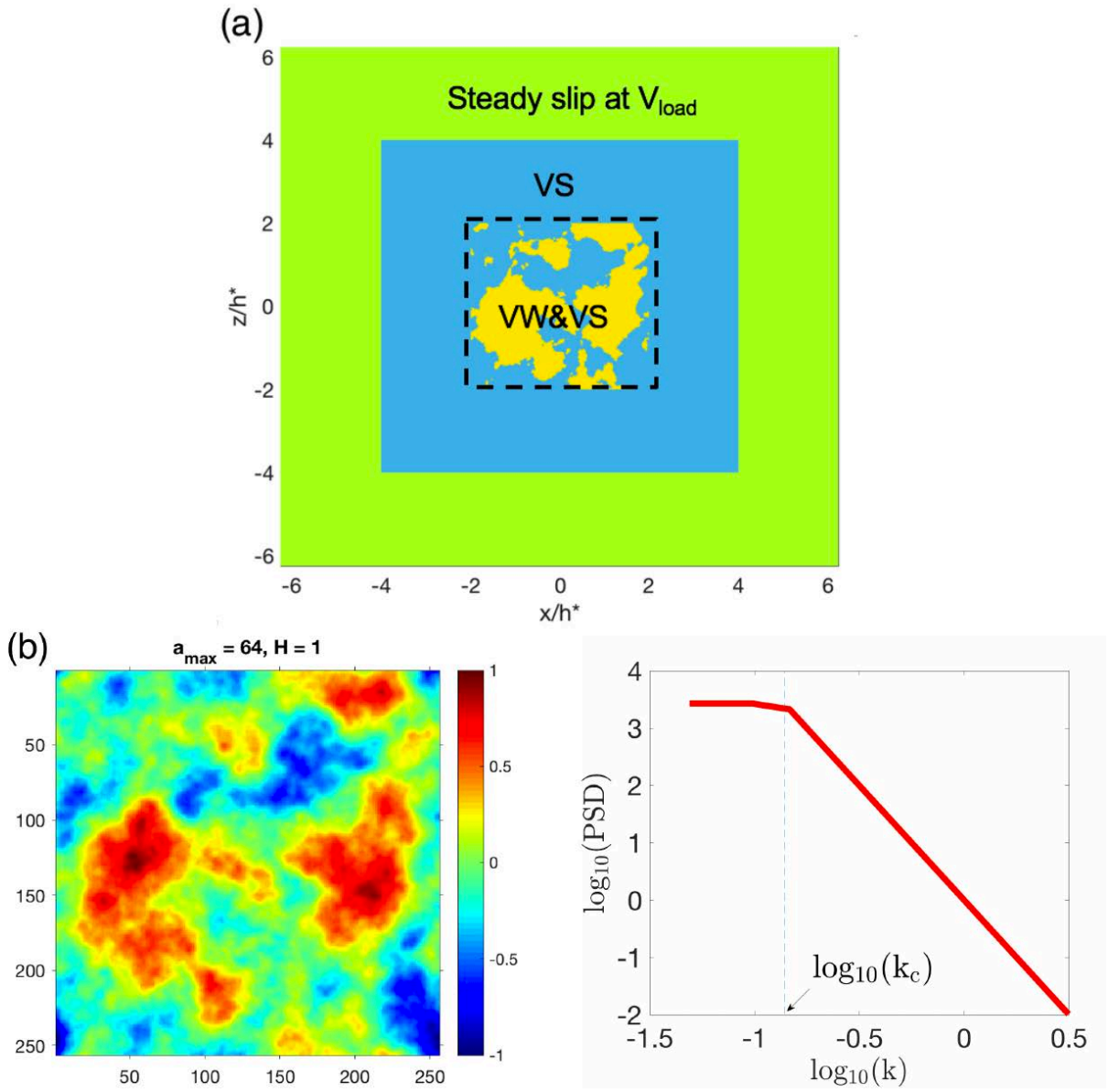

Figure 2: (a) Representative fault domain used in the simulations, normalized by the estimate of the nucleation size for the VW region (yellow), h^*. The region containing a distribution of VW and VS properties is surrounded by a VS region (blue), around which steady slip at V_{load} is applied (green) to simulate the steady creep of the larger surrounding region. (b) (Left) One realization of a random fractal field with two dominant areas that can serve as the source patches for the SF and LA sequences. (Right) Power spectral density of the fractal field, plotted in log scale. The dashed blue line indicates the corner wave number, $\log_{10} \mathrm{k_c} = -0.86$, beyond which the spectrum shows power-law decay.

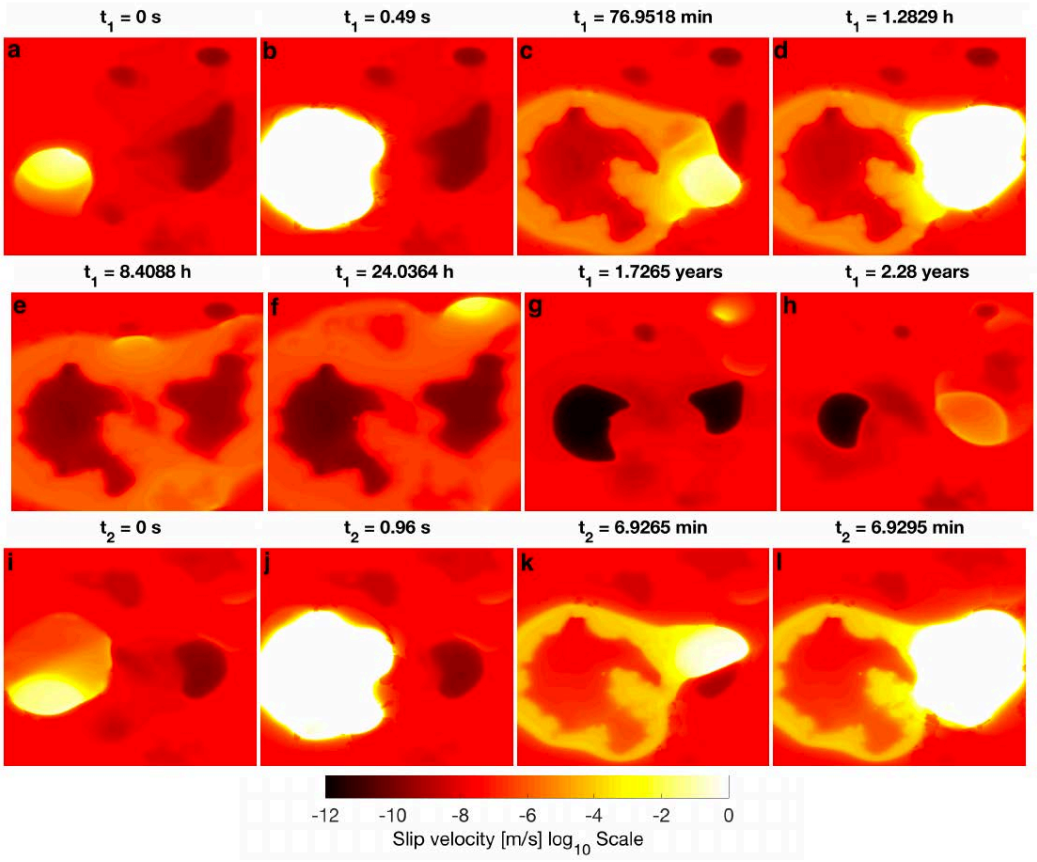

Figure 3: Slip velocity snapshots from the representative model that show the interaction between the two dominant patches. (a-b) An event nucleates in the (bigger) left patch. (c-d) The post-seismic slip front triggers the right patch and an event is nucleated there 1.3 hours later. (e-h) The perturbing patches and the smaller right patch host aseismic transients in the ensuing interseismic period, changing the prestress conditions before the following seismic events and hence contributing to the variability of slip. (i-j) Another event nucleates in the left patch. (k-l) The post-seismic slip front triggers the right patch, albeit with a shorter triggering time of about 7 minutes and nucleation at a different location, resulting in variable triggering times.

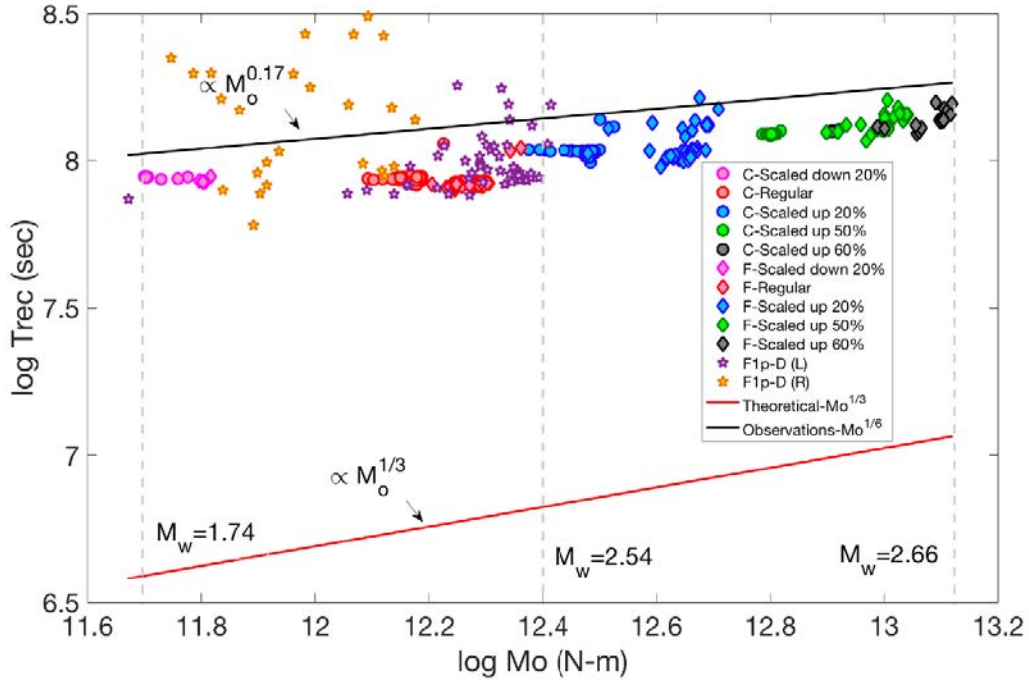

Figure 4: The modeling reproduces the observed scaling between the average recurrence time T_{rec} and average seismic moment M_o for the repeating events in our single patch circular models (circular markers), single patch fractal models (diamond markers), and two-patch fractal models (star markers). Results match qualitatively with the $T_{rec} - M_o$ observed at Parkfield (black line), approximated the expression by $T_{rec} \approx 7 \times 10^4$ (Chen and Lapusta, 2009). The theoretical $T_{rec} - M_o$ relation for a model with only seismic slip at the repeater locations and constant stress drops of 20 MPa is shown by the red line for comparison. The difference in the scaling exponent and the absolute values of the recurrence times between the theoretical model and our simulations is due to the presence of significant aseismic slip at the source locations (Chen and Lapusta, 2009; Lui and Lapusta, 2016), the fraction of which increases for smaller events, a factor not accounted for in the theoretical expression.

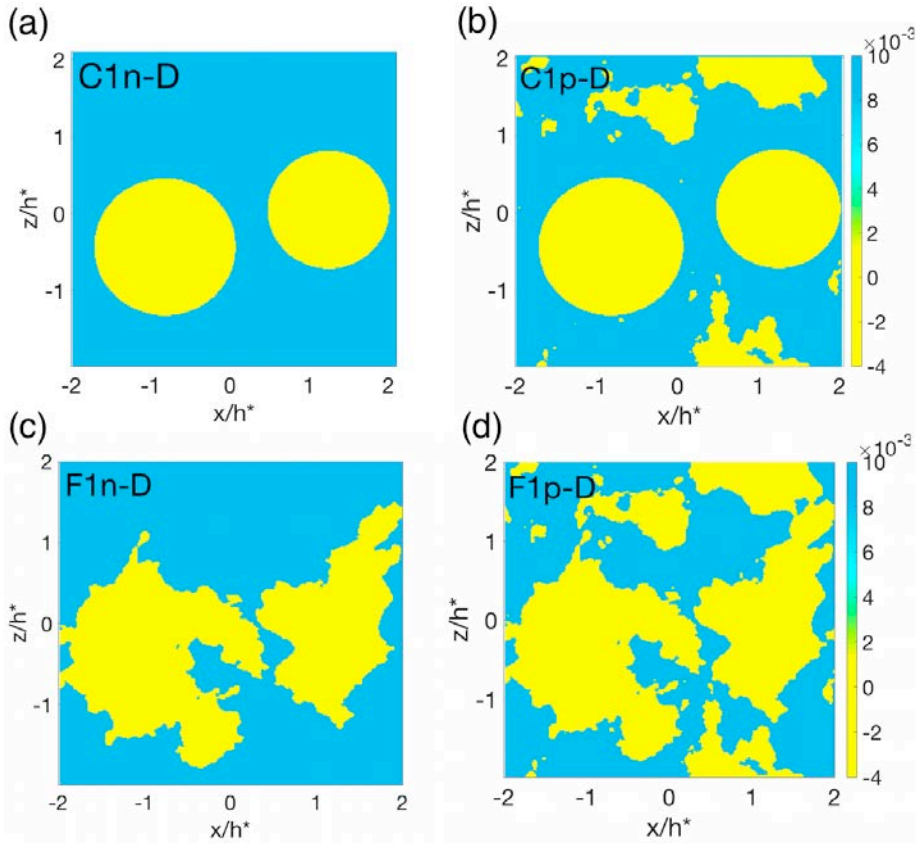

Figure 5: Fault models for the double patch simulations, C1n-D, C1p-D, F1n-D, F1p-D, where "D" stands for "double patches" and the color indicates the values of the velocity strengthening in the region surrounding the VW patches. The source patches can be circular (C) or fractal (F), with the following number (1, 2, or 3) corresponding to the VS value of $(a-b)_{VS} = 0.01, 0.004, 0.002$, respectively. "p" or "n" indicate that the other, smaller fractal VW patches are present or not. Our base model is F1p-D (panel d). To obtain model F1n-D (panel c), we take the F1p-D model, use image processing tools to identify the two largest patches, and remove the rest of the VW features. For comparison, we have a model with equivalent circular patches, C1n-D (panel a) which produces similar-sized events as the fractal patch models. The perturbing patches in the background of F1p-D are superposed on C1n-D to obtain C1p-D (panel b).

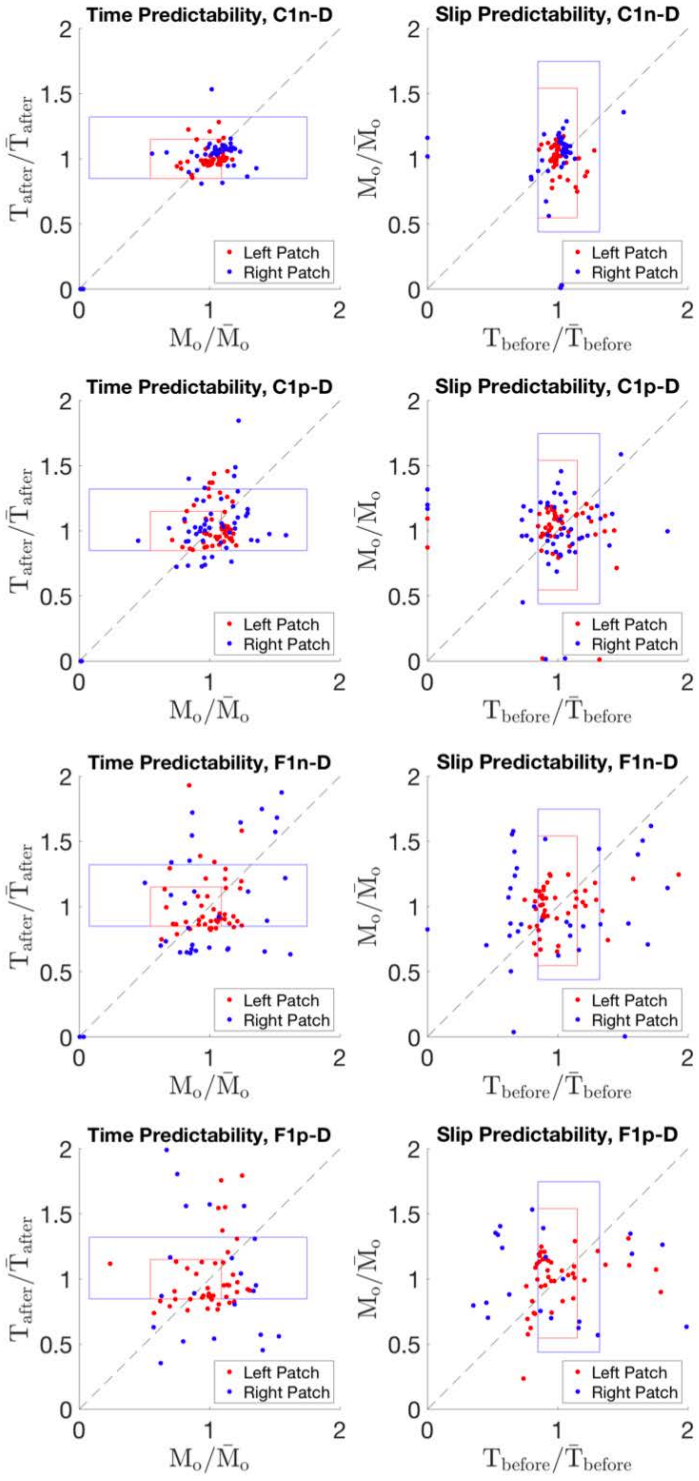

Figure 6: Slip-time predictability plots of the double patch models. The data points in the case of circular patch model (C1n-D) are clustered, whereas the addition of sub-critical perturbing patches is seen to increase the spread of data points (C1p-D). The change in source shape (F1n-D) significantly increases the scatter, which is further enhanced by addition of perturbing patches (F1p-D). The red and blue rectangle bounding the time- and slip-predictability data points of the SF-LA event pairs are superposed for comparison to models.

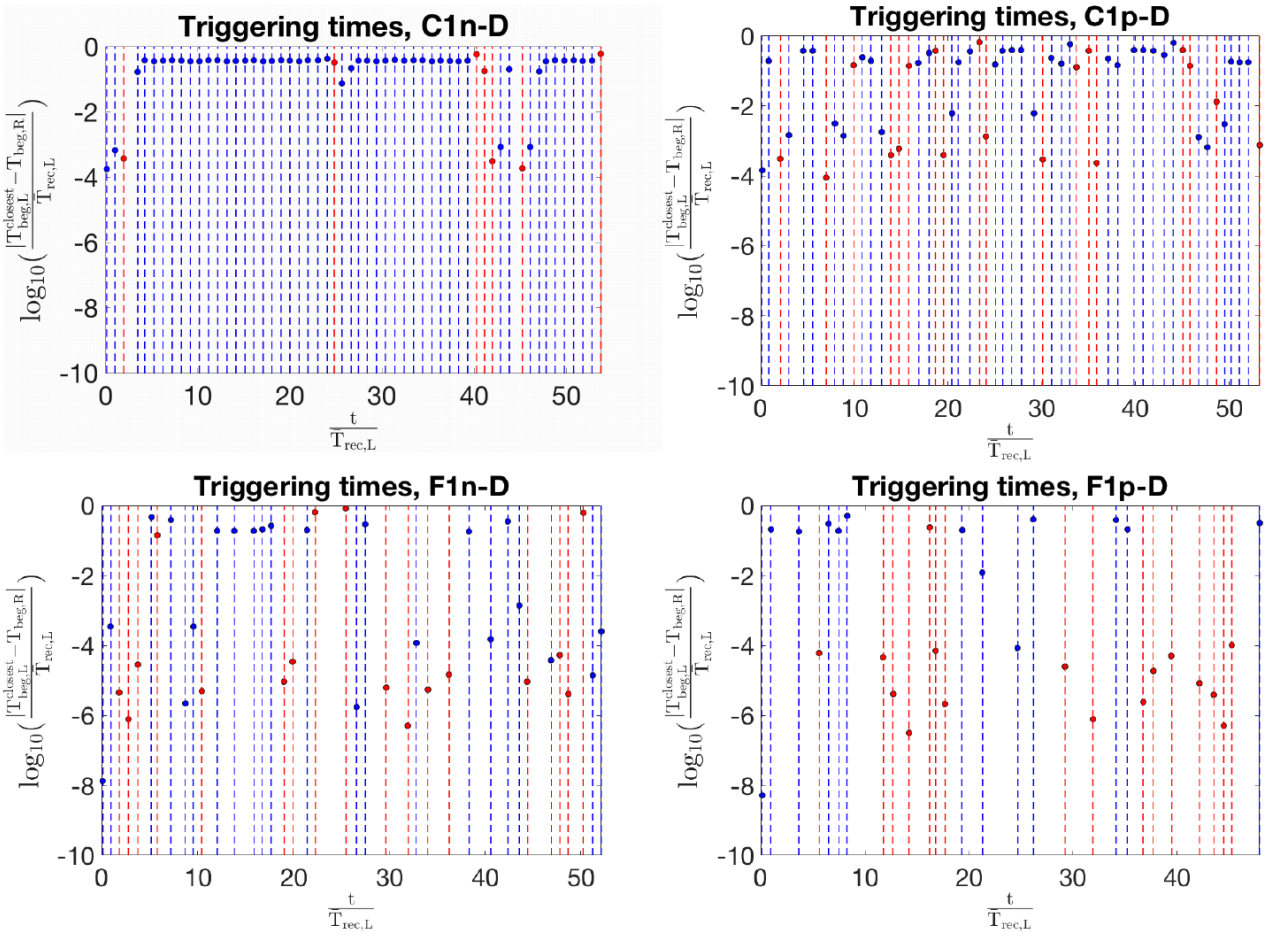

Figure 7: Triggering time distribution for double patch models. In the case of circular patch model (C1n-D), the shorter triggering times are absent, and the addition of sub-critical perturbing patches (C1p-D) is seen to slightly increase the range of data points, though still not to the extent of realistic behavior. The fractal source shape (F1n-D) gives rise to short triggering times, which persist with addition of perturbing patches (F1p-D).

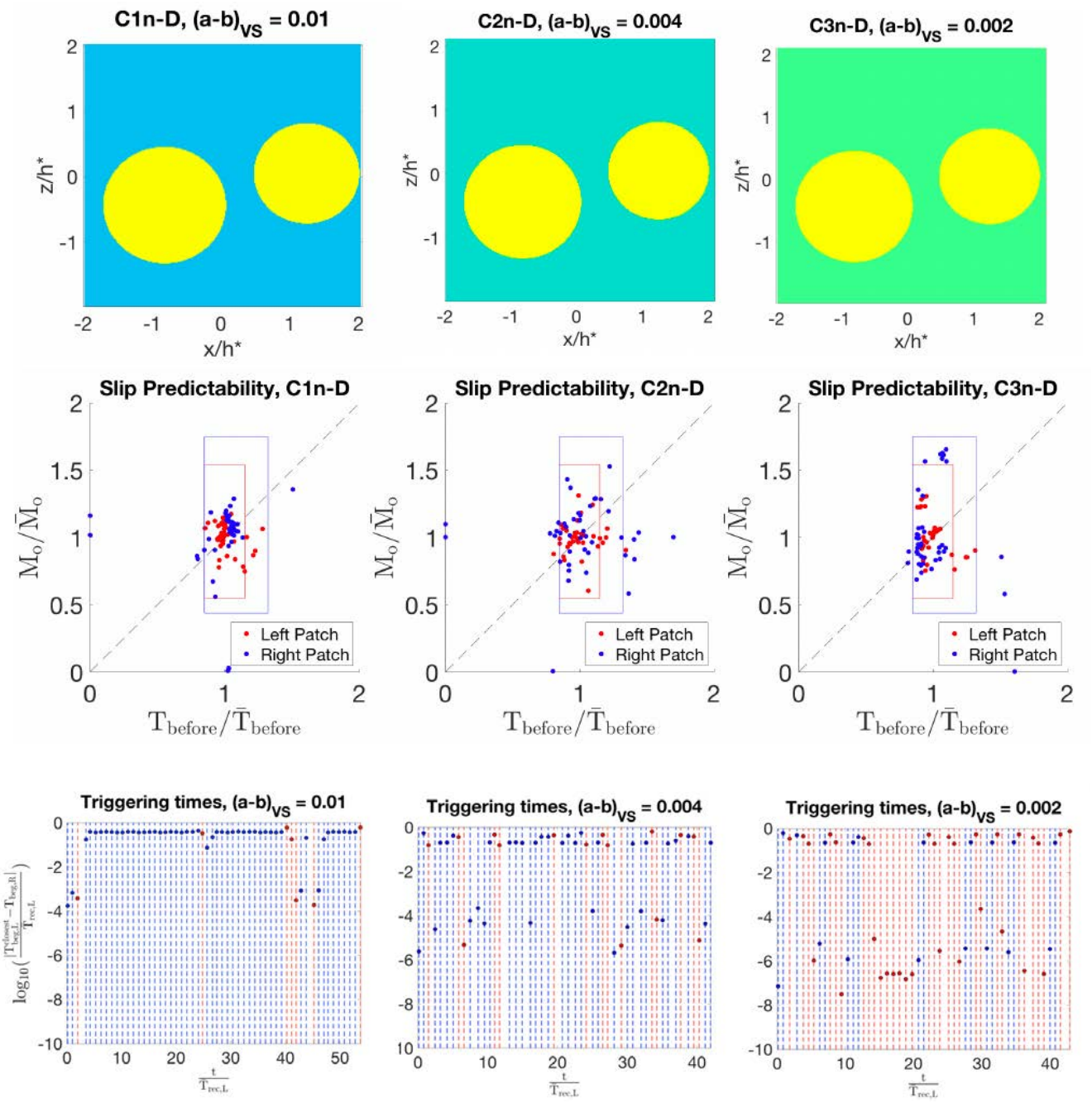

Figure 8: Slip-predictability plots and triggering time plots for models C1n-D, C2n-D, C3n-D with varying properties of the VS region. The spread of the seismic moment is seen to increase with the reduction in the strengthening of the VS medium in the slip-predictability plots, while the spread in recurrence times remains similar. The shorter triggering times are also introduced in the system by reducing the strengthening of the VS medium.

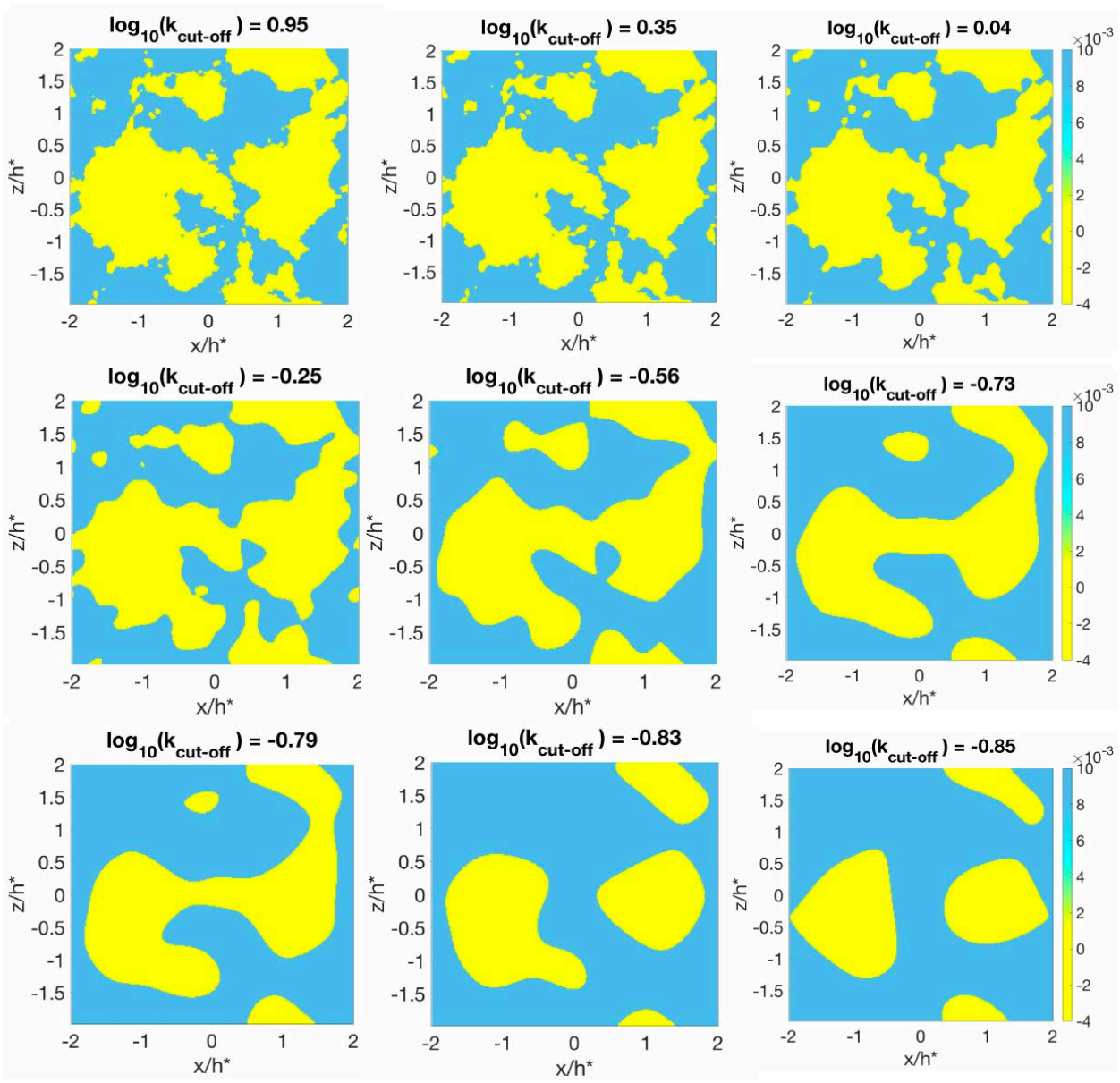

Figure 9: Smoothing of the patch shapes by eliminating high frequency contributions, above a cut-off wavenumber, $k_{cut-off}$. The fractal features gradually disappear, and the separate patches coalesce to form a single area. At $= -0.85$, just above corner wave number k_c (Figure 2b), the patch shapes become much simpler.

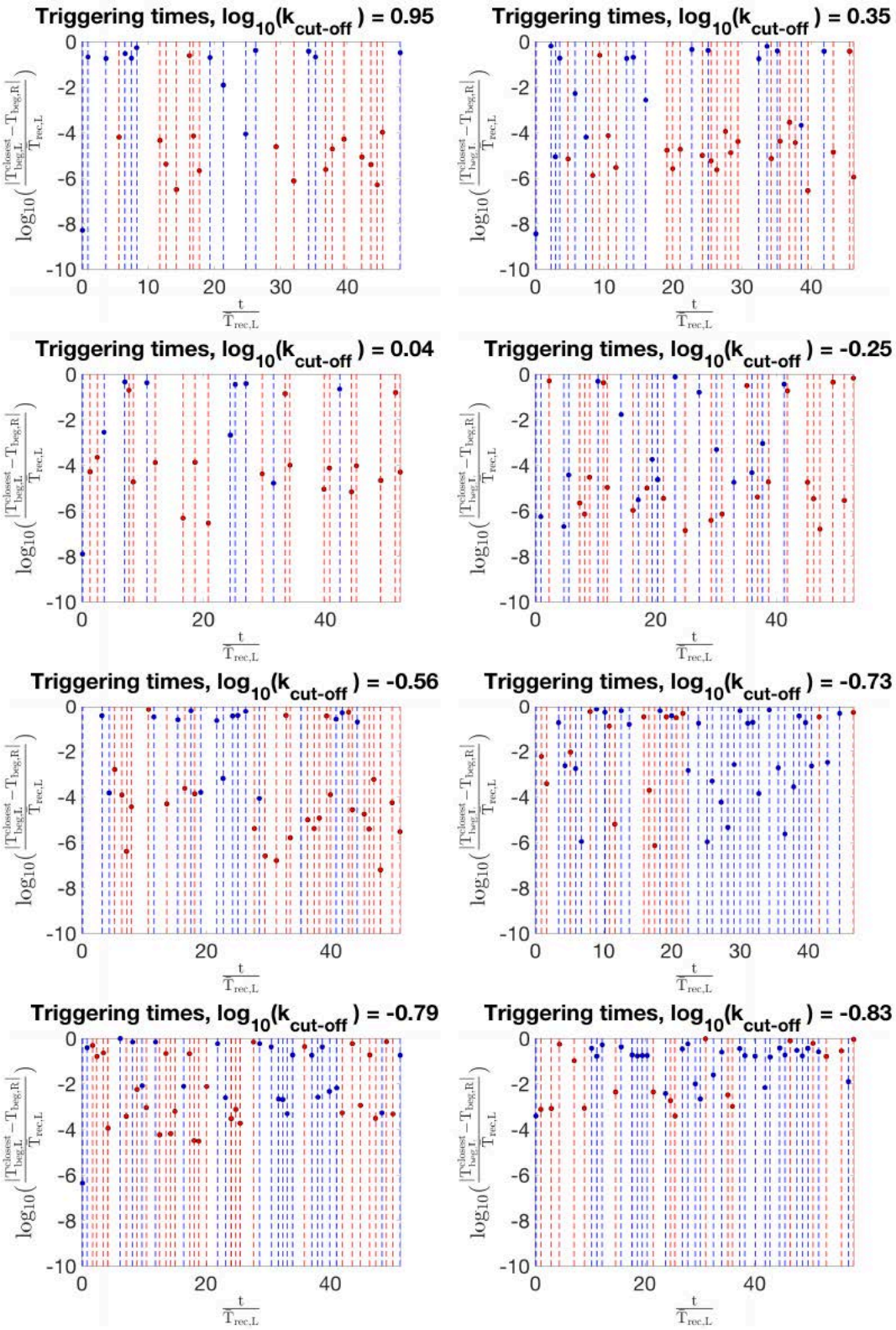

Figure 10: Triggering times in the models subjected to smoothing of fractal features. The short triggering times (1-100 s) vanish for smooth enough distributions, with the smoothest model having the response comparable to the model with circular patches.

3. Potential seismic rupture of the creeping segment

Our modeling related to the areas of Mw 7.6 1999 Chi-Chi earthquake and Mw 9.0 2011 Tohoku earthquake revealed that earthquake rupture may break through large portions of creeping segments, due to co-seismic thermal pressurization of pore fluids discussed in section 1 (Noda and Lapusta, 2013; Cubas et al., 2015). Allowing for such fault behavior results in a model that can explain, based on the same fault physics, a range of long-term and co-seismic observations about the area of the Tohoku earthquake, including more high-frequency radiation from areas of lower slip; the largest seismic slip in Tohoku earthquake occurring in a potentially creeping segment; the overall pattern of previous events in the area, including previous smaller events occurring below the area of the largest slip, and the complexity of Tohoku rupture, with propagation away from the trench first, then towards the trench, then away from the trench again (Noda and Lapusta, 2013; Cubas et al., 2015 and references therein).

Using prior USGS support, we successfully applied this paradigm to exploring the possibility of deeper slip in large earthquakes on the SAF (Jiang and Lapusta, 2016, 2017), suggesting that the segments with absence of concentrated microseismicity at the bottom of the traditionally defined seismogenic zone likely experienced such deeper penetration in the past. It is typically assumed that all seismic slip is confined within the seismogenic zone - often defined by the extent of the background seismicity or geodetically determined locking depth - with regions below creeping or deforming inelastically. Fault models based on standard rate-and-state laws support such assumptions, interpreting the locked zones as areas of VW properties that allow for earthquake nucleation, and the deeper creeping fault extensions as areas of VS properties that inhibit earthquake slip. However, enhanced co-seismic weakening of fault friction could be active not only in the VW part of the fault but also in the deeper VS fault extensions. As earthquake rupture penetrates into the creeping fault areas, it significantly increases slip rates there, potentially activating the co-seismic weakening and turning the stable fault areas into seismogenic ones. Observational studies have suggested that earthquake rupture could penetrate into the deeper creeping regions (Shaw and Wesnousky, 2008), and yet deep slip is difficult to detect due to limited resolution of source inversions with depth. Our simulations (Jiang and Lapusta, 2016, 2017) show that earthquakes indeed can penetrate into the deeper creeping fault extension, enabled by thermal pressurization at high slip rates for realistic fault properties. Depending on how deep coseismic slip reaches, the microseismicity at depth could be eliminated for most or all of the interseismic period (Figure 6) due to the stress concentration front being located below the low-rate VW zone that can nucleate small events. Our model predictions are consistent with the available seismic and geodetic observations of the Carrizo and Coachella segments on the San Andreas fault, where the depth of microseismicity is shallower than the geodetically estimated locking depth (Jiang and Lapusta, 2016).

The possibility that creeping segments - currently perceived as barriers – may generate large seismic slip and hence significantly enlarge the size of the expected event, as may have occurred in the Mw 9.0 2011 Tohoku earthquake, requires re-evaluation of seismic hazard in many areas, including California.

Under this award, we applied the developed fault models to explore the penetration of dynamic rupture into the creeping segment northwest of Parkfield due to shear-heating-induced thermal pressurization (TP) of pore fluids. We started by considering interaction with the creeping segments of the typical Parkfield earthquakes of Mw 6.0 for which we have developed a physical model that satisfies a range of available observations (Barbot et al., 2012); our constraint is that such events should arrest shortly after entering the creeping segment, as observed for the 2004 Mw event. We then considered the effect of incoming events with much larger slip that originate further southeast in the Carrizo segment and propagate into the Parkfield segment, and then into the creeping segment. Realistic modelling of this kind would require representing the nature of the connection between the Carrizo and Parkfield segments, which is not fully known and may be quite complex (e.g., Simpson et al., 2006). To examine the first-order effect of the size of the incoming rupture, we simply assumed a larger VW region to the right of the creeping region, generating events with larger slip. From equation (3), the efficiency of TP is in part controlled by the heat input τV, which in turn depends on the temporal and spatial dynamics of the incoming rupture and the properties of the creeping segment with which the rupture interacts; that is how

the size of the incoming rupture matters. Our study assumed that the dynamic slip entering the velocity-strengthening region is confined to one actively shearing zone; more complex scenarios can be considered in the future.

As the rapid slip penetrates into the creeping region due to inertial effects, the velocity-strengthening properties of the region make the shear stress τ increase, creating a competition between (a) larger dissipated energy and negative stress drop that may arrest the rupture and (b) the increased shear heating that can potentially activate TP given enough slip, creating dynamic weakening that may allow the rupture to carry on. The (evolving) value of slip rate V is also very important, as the shear heating has to be rapid enough to overcome the effects of the off-fault heat diffusion governed by thermal diffusivity α_{hy}. The highly nonlinear and coupled processes that govern the resulting evolution of slip can, at present, be only studied numerically, although we hope that our numerical experiments will lead to insights that will enable the simplified theoretical understanding of the phenomena. From the fault properties entering equation (3), ρc, Λ, and α_{th} are relatively well constrained (e.g., Rice, 2006; Noda and Lapusta, 2010, 2016) and, in our work, we use properties from past studies broadly representative of crustal faults. At the same time, the width w of the actively shearing zone which determines the shear heating rate $\omega(y)$ and the hydraulic diffusivity α_{hy} which determines whether the fluid can be trapped in the shear zone can vary by several orders of magnitude. We examined the values of w from the smallest proposed for an actively shearing zone, 0.1 mm (Rice, 2006), up to 10 mm. For the hydraulic diffusivity, we examined the values spanning from 10^{-5} m^2/s for well-healed dense rocks under significant compression (e.g., Rice, 2006; Noda and Lapusta, 2013 and references therein) to much larger values of 10^{-3} m^2/s for highly dynamically damaged and/or porous rocks under low compression.

We find that there is a range of dynamic weakening parameters for which Mw 6 events arrest in the creeping section, but larger, Mw 7.2 style events are able to propagate into the creeping section (Figures 11-12; Stephenson and Lapusta, manuscript in preparation). Of particular interest are the intermediate combinations of dynamic weakening parameters that do not allow Mw 6 events to propagate, but do allow Mw 7.2 events to rupture the entire creeping section, for example w =10 mm and $\alpha_{hy} = 10^{-4}$ mm^2/s (Fig. 11). Ruptures such as these could allow for the linking of the northern and southern parts of the San Andreas, allowing for much larger earthquakes. The identified sets of properties will serve as starting points for more sophisticated future studies in 3D models. We also plan to further develop our models to include the evolution in the shear zone width due to localization during rapid slip and evolution in the permeability due to co-seismic damage and interseismic healing, based on recent theoretical and experimental studies.

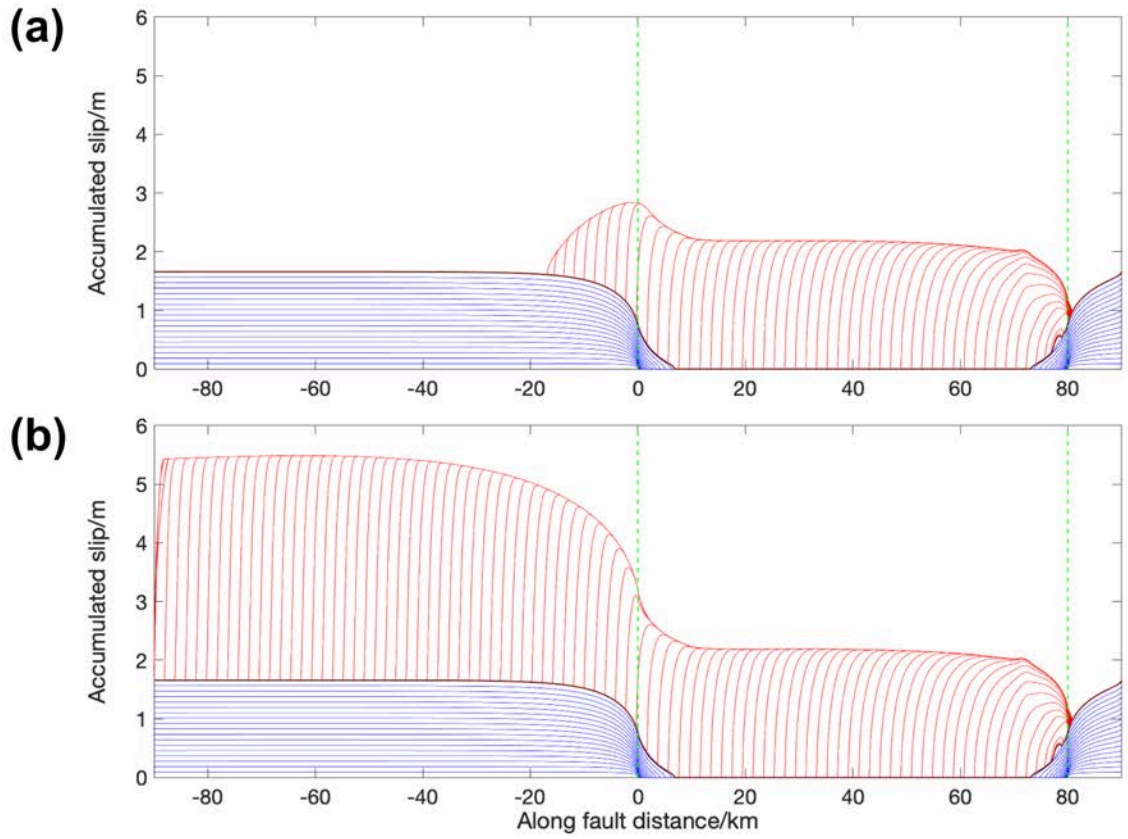

Figure 11. Simulations showing the effect of dynamic weakening on the penetration of Mw 7.2 style events into the creeping section. Blue lines indicate aseismic slip at two-year intervals. Red lines show seismic slip every 0.5 seconds. The 90-km-long creeping section is on the left-hand side of both figures. The green dashed lines indicate the boundary between the VS properties at low slip speeds on the left and the VW region to the right. (a) Less efficient dynamic weakening (w = 10 mm, $\alpha_{hy} = 10^{-3}$ mm^2/s) causes the left-going dynamic rupture event to rapidly die out after hitting the creeping section, limiting the event to approximately Mw 7.2. (b) With more efficient dynamic weakening (w = 10 mm, $\alpha_{hy} = 10^{-4}$ mm^2/s), a similar event ruptures through the entire 90 km creeping section in this model, creating a much larger earthquake. Note that Mw 6 style events rapidly arrest in the creeping section for both cases of dynamic weakening.

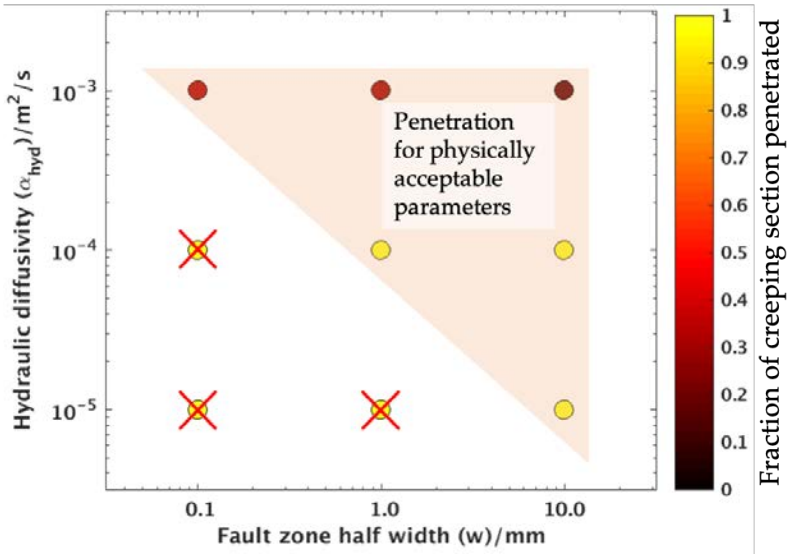

Figure 12. The fraction of the creeping section penetrated by Mw 7.2 style events for varying amounts of dynamic weakening, with its efficiency controlled by the hydraulic diffusivity and the fault zone width. On the bottom left, the three combinations of parameters marked with red crosses are ruled out as Mw 6 style events would also significantly penetrate into the creeping section with these properties, which is inconsistent with observations. The light orange triangle highlights parameters for which Mw 6 style events arrest almost at the boundary between the VW and VS segments, but Mw 7.2 events penetrate partially or completely through the creeping section.

9. REFERENCES

Abercrombie, R. E., Earthquake source scaling relationships from− 1 to 5 ML using seismograms recorded at 2.5 km depth, *J. Geophys. Res*., **100** (B12), 24015-24036, 1995.

Abercrombie, R. E., Stress drops of repeating earthquakes on the San Andreas Fault at Parkfield, *Geophys. Res. Lett.*, **41**, doi: 10.1002/2014GL062079, 2014.

Allmann, B. P., and P. M. Shearer, Spatial and temporal stress drop variations in small earthquakes near Parkfield, California, *J. Geophys. Res*., **112**, B04305, doi:10.1029/2006JB004395, 2007.

Allmann, B. P., and P. M. Shearer, Global variations of stress drop for moderate to large earthquakes. *J. Geophys. Res*., **114**(B1), B01310, doi:10.1029/2008JB005821, 2009.

Ampuero, J.-P., and A. M. Rubin, Earthquake nucleation on rate and state faults-Aging and slip laws, *J. Geophys. Res.*, **113**, B01302, doi:10.1029/2007JB005082, 2008.

Andrews, D. J., A fault constitutive relation accounting for thermal pressurization of pore fluid, *J. Geophys. Res*., **107**(B12), 2363, doi:10.1029/2002JB001942, 2002.

Baltay, A., S. Ide, G. Prieto, and G. Beroza, Variability in earthquake stress drop and apparent stress. *Geophys. Res. Lett.*, **38**(6)., 2011.

Barbot, S., N. Lapusta, and J.-P. Avouac, Under the hood of the earthquake machine: Toward predictive modeling of the seismic cycle, *Science*, *336*(6082), 707–710, doi:10.1126/science.1218796, 2012.

Bayart, E., A. M. Rubin, and C. Marone, Evolution of Fault Friction Following Large Velocity Jumps, *Eos Trans. AGU*, **87**(52), Fall Meet. Suppl., S31A-0180, 2006.

Beeler, N. M., T. E. Tullis, and J. D. Weeks , The roles of time and displacement in the evolution effect in rock friction, *Geophys. Res. Lett*., **21**, 1987–1990, 1994.

Beeler, N. M., D. L. Lockner, and S. H. Hickman, A simple stick-slip and creep-slip model for repeating earthquakes and its implication for microearthquakes at Parkfield, *Bull. Seismol. Soc. Am*., **91**, 1797–1804, 2001.

Beeler, N. M., and T. E. Tullis, Constitutive relationships for fault strength due to flash-heating. In: *2003 SCEC Annual Meeting Proceedings and Abstracts*, vol. 13, p. 66. Los, Angeles: Southern California Earthquake Center, Univ. of Southern California, 2003.

Beeler, N. M., T. E. Tullis, and D. L. Goldsby , Constitutive relationships and physical basis of fault strength due to flash-heating, *J. Geophys. Res*., **113**, B01401, doi:10.1029/2007JB004988, 2008.

Bhattacharya, P., Rubin, A. M., Bayart, E., Savage, H. M., & Marone, C., Critical evaluation of state evolution laws in rate and state friction: Fitting large velocity steps in simulated fault gouge with time-, slip-, and stress-dependent constitutive laws. *J. Geophys. Res.*, **120,** 9, 6365-6385, 2015.

Bizzarri, A., and M. Cocco, A thermal pressurization model for the spontaneous dynamic rupture propagation on a three-dimensional fault: 1. Methodological approach, *J. Geophys. Res*., **111**, B05303, doi:10.1029/2005JB003862, 2006a.

Bizzarri, A., and M. Cocco, A thermal pressurization model for the spontaneous dynamic rupture propagation on a three-dimensional fault: 2. Traction evolution and dynamic parameters, *J. Geophys. Res*., **111**, B05304, doi:10.1029/2005JB003864, 2006b.

Blanpied, M. L., D. A. Lockner and J. D. Byerlee, Fault stability inferred from granite sliding experiments at hydrothermal conditions, *Geophys. Res. Letters*, **18** (4), 609-612, 1991.

Blanpied, M. L., D. A. Lockner and J. D. Byerlee, Frictional slip of granite at hydrothermal conditions, *J. Geophys. Res*., **100**, 13045-13064, 1995.

Brodsky, E. E., J.J. Gilchrist, A. Sagy, C. Collettini, Faults smooth gradually as a function of slip, *Earth and Planetary Science Letters,* 302, 185-193, 2011.

Brune, J., Tectonic stress and the spectra of seismic shear waves from earthquakes, *J. Geophys. Res.*, **75**, 4997–5009, doi:10.1029/JB075i026p04997, 1970.

Brune, J. N., Correction, *J. Geophys. Res.*, **76**, 5002, 1971.

Bürgmann, R., D. Schmidt, R. M. Nadeau, M. d'Alessio, E. Fielding, D. Manaker, T. V. McEvilly, and M. H. Murray, Earthquake potential along the northern Hayward fault, California, *Science*, **289**, 1178–1182, 2000.

Carpenter, B. M., C. Marone, and D. M. Saffer, Frictional behavior of materials in the 3D SAFOD volume, Geophys. Res. Lett., 36, L05302, doi:10.1029/2008GL036660, 2009.

Chen, K. H., R. M. Nadeau, and R.-J. Rau, Towards a universal rule on the recurrence interval scaling of repeating earthquakes?, *Geophys. Res. Lett*., **34**, L16308, doi:10.1029/2007GL030554, 2007.

Chen, K. H., Bürgmann, R., and Nadeau, R. M., Do repeating earthquakes talk to each other?, *EOS Trans. AGU*, S33C-1469, 2007.

Chen, T., and N. Lapusta , Scaling of small repeating earthquakes explained by interaction of seismic and aseismic slip in a rate and state fault model, *J. Geophys. Res.*, 114, B01311, doi:10.1029/2008JB005749, 2009.

Chen, K. H., R. Bürgmann, R. M. Nadeau, T. Chen, and N. Lapusta, Postseismic variations in seismic moment and recurrence interval of repeating earthquakes, *Earth Planet. Sci. Lett.*, 299, doi:10.1016/j.epsl.2010.08.027, 118–125, 2010.

Cubas, N., N. Lapusta, J.-P. Avouac, H. Perfettini, Numerical modeling of long-term earthquake sequences on the NE Japan megathrust: Comparison with observations and implications for fault friction, *Earth Planet. Sci. Lett.*, 419, 2015.

Dieterich, J. H., Modeling of rock friction- 1 Experimental results and constitutive equations, *J. Geophys. Res.*, **84**, 2161-2168, 1979.

Dieterich, J. H., Constitutive properties of faults with simulated gouge, in *Mech. Beh. Crustal Rocks*, Geophys. Monogr. Ser., **24**, ed. by N. L. Carter, M. Friedman, J. M. Logan and D. W. Stearns, AGU, Washington, DC, 103-120, 1981.

Dieterich, J. H. Applications of rate- and state-dependent friction to models of fault slip and earthquake occurrence. In Kanamori, H. (ed.) *Treatise on Geophysics*, **4**, chap. 4, 107–129 (Elsevier, Amsterdam, 2007).

Dreger, D., R. M. Nadeau, and A. Chung, Repeating earthquake finite source models: Strong asperities revealed on the San Andreas Fault. *Geophys. Res. Lett.*, **34**(23), L23302, doi:10.1029/2007GL031353 2007.

Ellsworth, W. L. and L. D. Dietz, Repeating earthquakes: characteristics and implications, Proc. of Workshop 46, the 7th U.S.-Japan Seminar on Earthquake prediction, U.S.Geol.Surv. Open-File Rept. 90-98, 226-245, 1990.

Gladwin, M. T., R. L. Gwyther, R. H. G. Hart, and K. S. Breckenbridge, Measurements of the Strain Field Associated with Episodic Creep Events on the San Andreas Fault at San Juan Bautista, California, *Journal of Geophysical Research*, 99, 4559-4565, 1994.

Goldsby, D. L., and T. E. Tullis, Flash heating/melting phenomena for crustal rocks at (nearly) seismic slip rates. In: *2003 SCEC Annual Meeting Proceedings and Abstracts*, vol. 13, p. 98-99. Los Angeles: Southern California Earthquake Center, Univ. of Southern California, 2003.

Goldsby, D. L. and T. E. Tullis, Flash heating leads to low frictional strength of crustal rocks at earthquake slip rates, *Science*, **334**, 216-218, DOI: 10.1126/science.1207902, 2011.

Hauksson, E., W. Yang, and P. M. Shearer, Waveform Relocated Earthquake Cat- alog for Southern California (1981 to June 2011), *Bull. Seis. Soc. Amer.*, *102*(5), 2239– 2244, 2012.

Hickman, S., M. Zoback, and W. Ellsworth, Introduction to special section: Preparing for the San Andreas Fault Observatory at depth, *Geophys. Res. Lett*., **31**, L12S01, doi:10.1029/2004GL020688, 2004.

Hori, T., N. Kato, K. Hirahara, T. Bada, and Y. Kaneda, A numerical simulation of earthquake cycles along the Nankai trough, southwest Japan: Lateral variation in frictional property due to slab geometry controls the nucleation position, *Earth. Planet. Sci. Lett.*, 228, 215-226, 2004.

Ide, S., and G. C. Beroza, Does apparent stress vary with earthquake size. *Geophys. Res. Lett.,* **28**(17), 3349-3352, 2001.

Igarashi, T., Matsuzawa, T., and A. Hasegawa, Repeating earthquakes and interplate aseismic slip in the northeastern Japan subduction zone, *J. Geophys. Res.* 108, B5, 2249, 2003.

Imanishi, K., W. L. Ellsworth, S. G. Prejean, Earthquake source parameters determined by the SAFOD Pilot Hole seismic array, *Geophys. Res. Letters*, **31**, L12S09, doi:10.1029/2004GL019420, 2004.

Jeppson, T. N., K. K. Bradbury, and J. P. Evans, Geophysical properties within the San Andreas Fault Zone at the San Andreas Fault Observatory at Depth and their relationships to rock properties and fault zone structure, *J. Geophys. Res.*, **115**, B12423, 2010.

Jiang, J., and N. Lapusta, Deeper penetration of large earthquakes on seismically quiescent faults, *Scienc*e, 352, 2016.

Jiang, J., and N. Lapusta, Connecting the depth limits of interseismic locking, microseismicity, and large earthquakes in models of long-term fault slip, submitted to *J. Geophys. Res.,* in revision, 2017.

Kanamori, H., & Anderson, D. L. Theoretical basis of some empirical relations in seismology. *Bull. Seismol. Soc. Am.*, **65** (5), 1073-1095, 1975.

Kaneko, Y., and P. M. Shearer, Seismic source spectra and estimated stress drop derived from cohesive-zone models of circular subshear rupture. *Geophys. J. Int.*, **197**, 1002-1015, 2014.

Kaneko, Y., and P. M. Shearer, Variability of seismic source spectra, estimated stress drop, and radiated energy, derived from cohesive zone models of symmetrical and asymmetrical circular and elliptical ruptures. *J. Geophys. Res*, **120**(2), 1053-1079, 2015.

Kato, N., and T. E. Tullis, A composite rate- and state-dependent law for rock friction, *Geophys. Res. Lett.*, 28, 1103–1106, 2001.

Lapusta, N., and Y. Liu, 3D boundary-integral modeling of spontaneous earthquake sequences and aseismic slip, accepted for publication, *J. Geophys. Res.*, 2009.

Lin, Y., and N. Lapusta, Microseismicity simulated on heterogeneous faults: on scaling of seismic moment with duration and seismological estimates of stress drops, submitted to *Geophys. Res. Lett.,* 2018.

Lockner, D. A., C. Morrow, D. Moore, and S. Hickman, Low strength of deep San Andreas fault gouge from SAFOD core, *Nature*, **472**, 82-85, 2011.

Lui, S.K.Y., and N. Lapusta, Repeating microearthquake sequences interact predominantly through postseismic slip, *Nature Comm*, doi: 10.1038/ncomms13020, 2016.

Lui, S. K., and N. Lapusta, Modeling high stress drops, scaling, interaction, and irregularity of repeating earthquake sequences near Parkfield, *J. Geophys. Res: Solid Earth* 123, no. 12 (2018): 10-854

Madariaga, R., Dynamics of an expanding circular crack, *Bull. Seismol. Soc. Am.*, **66**, 639–666, 1976.

Mai, P. M., & Beroza, G. C. A spatial random field model to characterize complexity in earthquake slip. *J. Geophys. Res.*, **107** (B11), 2002.
Marone, C. , Laboratory-derived friction laws and their application to seismic faulting, Ann. *Rev. Earth Planet. Sci*., **26**, 643– 696, 1998.
Marone, C., Vidale, J. E., and W. L. Ellsworth, Fault healing inferred from time-dependent variations in-source properties of repeating earthquakes, *Geophys. Res. Lett.,* 22, 3095-3098, 1995.
Matsubara, M., Y. Yagi, and K. Obara, Plate boundary slip associated with the 2003 off-Tokachi earthquake based on small repeating earthquake data, *Geophys. Res. Lett*., **32**, L08316, doi:10.1029/2004GL022310, 2005.
Maurer, J., and K. M. Johnson, Fault coupling and potential for earthquakes on the creeping section of the Central San Andreas Fault, *J. Geophys. Res.*, 119, 4414-4428, 2014.
Nadeau, R. M., and L. R. Johnson, Seismological studies at Parkfield VI: Moment release rates and estimates of source parameters for small repeating earthquakes, *Bull. Seism. Soc. Am.,* 88, 1998.
Nadeau, R. M., and T. V. McEvilly, Fault slip rates at depth from recurrence intervals of repeating microearthquakes, *Science*, **285**, 718–721, 1999.
Nadeau, R. M., and T, V. McEvilly, Periodic Pulsing of Characteristic Microearthquakes on the San Andreas Fault, *Science*, 303, 220-223, 2004.
Nadeau, R. M., A. Michelini, R. A. Uhrhammer, D. Dolenc, T. V. McEvilly, Detailed kinematics, structure and recurrence of micro-seismicity in the SAFOD target region, *Geophys. Res. Letters*, **31**, L12S08, doi:10.1029/2003GL019409, 2004.
Noda, H., E. M. Dunham, and J. R. Rice, Earthquake ruptures with thermal weakening and the operation of major faults at low overall stress levels, *J. Geophys. Res.*, *114*, B07302, doi:10.1029/2008JB006143, 2009.
Noda, H., and N. Lapusta, Three-dimensional earthquake sequence simulations with evolving temperature and pore pressure due to shear heating: Effect of heterogeneous hydraulic diffusivity, *J. Geophys. Res.*, *115*(B12), doi:10.1029/2010JB007780, 2010.
Noda, H., and N. Lapusta, Stable creeping fault segments can become destructive as a result of dynamic weakening, *Nature*, 1–6, doi:10.1038/nature11703, 2013.
Perrin, G., J. R. Rice, and G. Zheng, Self-healing slip pulse on a frictional surface, *J. Mech. Phys. Solids*, **43**, 1461-1495, 1995.
Rice, J. R. and A. L. Ruina, Stability of steady frictional slipping, *J. Appl. Mech.*, **50**, 343-349, 1983.
Rice, J. R., Heating and weakening of faults during earthquake slip, *J. Geophys. Res*., doi:10.1029/2005JB004006, 2006.
Rice, J. R., N. Lapusta, and K. Ranjith, Rate and state dependent friction and the stability of sliding between elastically deformable solids, *J. Mech. Phys. Solids* 49, 1865-1898, 2001.
Rubin, A.M., and J.-P. Ampuero, Earthquake nucleation on (aging) rate and state faults, *J. Geophys. Res.,* 110, doi:10.1029/2005JB003686, 2005.
Rubinstein, J.L., W.L. Ellsworth, K.H. Chen, and N. Uchida, The time and slip-predictable models cannot be dependably used to predict earthquake behavior 1: Repeating earthquakes, *J. Geophys. Res.,*117, B02306, doi:10.1029/2011JB008724, 2012.
Ruina, A. L., Slip instability and state variable friction laws, *J. Geophys. Res*., **88**, 10359-10370, 1983.
Sammis, C. G., Nadeau, R. M., & Johnson, L. R. How strong is an asperity?. *J. Geophys Res*, **104** (B5), 10609-10619, 1999.
Sammis, C. G., and J. R. Rice, Repeating earthquakes as low-stress-drop events at a border between locked and creeping fault patches, *Bull. Seism. Soc. Am.,* 91, 3, 532-537, 2001.
Sato, T., and T. Hirasawa, Body wave spectra from propagating shear cracks, *J. Phys. Earth*, **21**, 415–431, 1973.
Schaff, D. P., and G. C. Beroza, Coseismic and postseismic velocity changes measured by repeating earthquakes, *J. Geophys. Res*., **109**, B10302, doi:10.1029/2004JB003011, 2004.
Schaff, D. P., G. C. Beroza, and B. E. Shaw, Postseismic response of repeating aftershocks, *Geophys. Res. Lett*., **25**, 4549– 4552, 1998.
Scholz, C. H. Earthquakes and friction laws. *Nature* **391**, 37–42, 1998.
Schulz, S. S., Catalog of Creepmeter Measurements in California from 1966 through 1988, USGS Open-File Report. USGS, 1989.

Shaw, B. E., and S. G. Wesnousky, Slip-Length Scaling in Large Earthquakes: The Role of Deep-Penetrating Slip below the Seismogenic Layer, *Bull. Seismol. Soc. Amer.*, *98*(4), 1633–1641, doi:10.1785/0120070191, 2008.

Shelly, D. R., & Johnson, K. M. Tremor reveals stress shadowing, deep postseismic creep, and depth-dependent slip recurrence on the lower-crustal San Andreas fault near Parkfield. *Geophysical Research Letters*, **38** (13), 2011.

Shelly, D. R. Complexity of the deep San Andreas Fault zone defined by cascading tremor. *Nature Geoscience*, **8**(2), 145-151, 2015.

Sibson, R. H., Interaction between temperature and pore-fluid pressure during earthquake faulting and a mechanism for partial or total stress relief, *Nature*, **243**, 66–68, 1973.

Simpson, R. W., M. Barall, J. Langbein, J. R. Murray, and M. J. Rymer, San Andreas Fault geometry in the Parkfield, California, region, *Bull. Seis. Soc. Amer.*, *96*(4B), doi:10.1785/0120050824, 2006.

Tullis, T. E., Friction of Rock at Earthquake Slip Rates, in *Treatise on Geophysics*, vol. 4, Earthquake Seismology, edited by H. Kanamori, Elsevier, Amsterdam, 2007.

Tsutsumi, A. & Shimamoto, T. High velocity frictional properties of gabbro, *Geophys. Res. Lett.* **24**, 699–702, 1997.

Vidale, J. E., Ellsworth, W. L., Cole, A., and C. Marone, Variations in rupture process with recurrence interval in a repeated small earthquake, *Nature*, 368, 6472, 624-626, 1994.

Waldhauser, Felix, and David P. Schaff, Large-scale relocation of two decades of Northern California seismicity using cross-correlation and double-difference methods, *Journal of Geophysical Research: Solid Earth* 113.B8, 2008.

Zoback, M., S. Hickman, and W. Ellsworth, Scientific Drilling Into the San Andreas Fault Zone, *Eos Trans. AGU*, **91**, 197-198, 2010.

Project data: Describe how the data will be made publicly available

This project produced numerical data from simulations that was analyzed and processed into tables, figures, and movies, which are being included in manuscripts that we are preparing for publication (please see the list below). To make the produced data publicly available and maximize potential for reuse, we will store the data products obtained under this project in the Caltech Collection of Open Digital Archives (CODA) which gives all records and datasets permanent URLs and Digital Object Identifiers (DOIs). Caltech CODA is indexed by all major Internet search engines. We will also provide and store on CODA the additional documentation to make the data understandable and usable by others (e.g., README files), MATLAB and Python scripts to open and process the data. CODA is a secure institutional repository that conforms to international standards. The investigations and analyses based on the data will be published in the peer-reviewed literature, with the CODA URLs and DOIs for the data included in the publications.

Publications and presentations resulting from the work performed under the award

Stephenson, O, and N. Lapusta, Exploring the Possibility of Dynamic Rupture Through the Creeping Section of the San Andreas Fault in a Simplified 2D Model, manuscript in preparation, to be submitted in 2021.

Sudhir, K., and N. Lapusta, Modeling the variability of repeating earthquake sequences on rate-and-state interfaces: realistic shapes of source patches vs. properties of the creeping region, manuscript in preparation, to be submitted in 2020.

Stephenson, O, and N. Lapusta, Simplified Elastodynamic Modeling of Potential Dynamic Rupture Through Creeping Fault Sections, 7th Int. Conf. on Coupled THMC Processes in Geosystems, Utrecht, the Netherlands, July 2019.

Sudhir, K., and N. Lapusta, Computational Modeling of Slip Patterns on Heterogeneous Frictional Interfaces, Engineering Mechanics Institute Conference, Pasadena, CA, June 2019.

Sudhir, K., and N. Lapusta, Computational Modeling of Slip Patterns on Heterogeneous Frictional Interfaces, Symposium on The Applications of Mechanics to Geophysics, University of California, San Diego, La Jolla, CA, June 2019.

Sudhir, K., and N. Lapusta, Realistic variability in seismic moment and recurrence time of repeating earthquakes reproduced in models with fractal shapes of fault patches, 2019 SCEC Annual Meeting, Palm Springs, CA, Sept. 2019.

Sudhir, K., and N. Lapusta, Realistic Variability in Seismic Moment and Recurrence Time of Repeating Earthquakes Reproduced in Models with Fractal Heterogeneity in Friction Properties, AGU Fall meeting, San Francisco, CA, Dec. 2019.